Title

Orogenic Propagating Precipitation Systems over the United States in a Global Climate Model with Embedded Explicit Convection

Journal

Journal of the Atmospheric Sciences, 68(8)

ISSN

0022-4928 1520-0469

Authors

Pritchard, Michael S
Moncrieff, Mitchell W
Somerville, Richard C. J

Publication Date

2011-08-01

DOI

10.1175/2011JAS3699.1

Orogenic Propagating Precipitation Systems over the United States in a Global Climate Model with Embedded Explicit Convection

MICHAEL S. PRITCHARD

Scripps Institution of Oceanography, University of California, San Diego, La Jolla, California

MITCHELL W. MONCRIEFF

National Center for Atmospheric Research, Boulder, Colorado

RICHARD C. J. SOMERVILLE

Scripps Institution of Oceanography, University of California, San Diego, La Jolla, California

(Manuscript received 12 October 2010, in final form 8 February 2011)

ABSTRACT

In the lee of major mountain chains worldwide, diurnal physics of organized propagating convection project onto seasonal and climate time scales of the hydrologic cycle, but this phenomenon is not represented in conventional global climate models (GCMs). Analysis of an experimental version of the superparameterized (SP) Community Atmosphere Model (CAM) demonstrates that propagating orogenic nocturnal convection in the central U.S. warm season is, however, representable in GCMs that use the embedded explicit convection model approach [i.e., multiscale modeling frameworks (MMFs)]. SP-CAM admits propagating organized convective systems in the lee of the Rockies during synoptic conditions similar to those that generate mesoscale convective systems in nature. The simulated convective systems exhibit spatial scales, phase speeds, and propagation speeds comparable to radar observations, and the genesis mechanism in the model agrees qualitatively with established conceptual models. Convective heating and condensate structures are examined on both resolved scales in SP-CAM, and coherently propagating cloud ''metastructures'' are shown to transcend individual cloud-resolving model arrays. In reconciling how this new mode of diurnal convective variability is admitted in SP-CAM despite the severe idealizations in the cloud-resolving model configuration, an updated discussion is presented of what physics may transcend the re-engineered scale interface in MMFs. The authors suggest that the improved diurnal propagation physics in SP-CAM are mediated by large-scale first-baroclinic gravity wave interactions with a prognostic organization life cycle, emphasizing the physical importance of preserving ''memory'' at the inner resolved scale.

1. Introduction

Projections of future rainfall by current generation global climate models (GCMs) are especially uncertain in continental interiors during the warm season. The 2007 Fourth Assessment Report (AR4) of the Intergovernmental Panel on Climate Change (IPCC) shows that the ensemble of conventional GCMs cannot even agree on the sign of rainfall changes in these heavily populated parts of the world.

A fundamental reason for this inadequacy is that conventional GCMs cannot capture the physics of diurnally propagating organized mesoscale convective systems (MCSs). In nature, such systems deliver much of the warm seasonal mean rainfall to the continental interior in the lee of topography (Laing and Fritsch 1997). In the central United States as much as half of summer rain is linked to these eastward propagating systems originating over the Rockies (Jiang et al. 2006). However, in atmospheric climate models MCSs are below the affordable grid resolution for climate-scale integration and are not properly represented by statistical cumulus parameterization schemes (Moncrieff and Liu 2006). These parameterizations are generally cast rigidly in terms of a local buildup (usually within intervals of

Corresponding author address: Michael S. Pritchard, Scripps Graduate Department, 9500 Gilman Dr., Mail Code 0224, La Jolla, CA 92093–0224.
E-mail: mikepritchard@ucsd.edu

DOI: 10.1175/2011JAS3699.1

15–60 min) of instability metrics such as convective available potential energy (CAPE). Thus they cannot admit nonlocal diurnal convective physics governing MCS organization and propagation in nature, which take place over several hours and involve nonequilibrium, often nonlocal, physics. As a result, the ensemble members of the AR4 GCMs do not simulate propagating episodes of convection and disagree wildly about precipitation trends in the lee of mountains, such that there is low confidence in long-term projections of seasonal-to-climate-scale rainfall variations over continents around the world.

The above issues associated with convective parameterization in climate models are in stark contrast to the successful simulation of MCS-type organization afforded by (nonhydrostatic) cloud-system-resolving models (CRMs) with a computational mesh of about 1 km. This success is summarized in the review paper on MCSs by Houze (2004), and on cloud-system models by Tao and Moncrieff (2009). In particular, Moncrieff and Liu (2006) showed that MCSs initiated over the Continental Divide and their subsequent eastward propagation were reliably simulated by a cloud-resolving model, as comparisons of simulated precipitation with radar measurements indicated.

An experimental new approach for treating subgrid convective effects in GCMs offers an alternate path for improving climate projections in these difficult to simulate parts of the atmosphere. Multiscale modeling frameworks (MMFs) are GCMs that use thousands of embedded idealized 2D cloud process resolving model arrays to calculate subgrid cloud and boundary layer adjustments to resolved dynamics, instead of conventional statistical parameterizations (Randall et al. 2003). The idea traces back to Grabowski and Smolarkiewicz (1999) and is designed to leverage recent increases in the number and speed of processing elements in modern supercomputer clusters without introducing the parallel overhead that historically limits the computational scale of conventional global climate simulations. Only a handful of multiscale models currently exist, which are largely experimental and in their infancy. Problems exist in their mean cloud and rainfall distribution (Khairoutdinov et al. 2005; Marchand et al. 2009; Zhang et al. 2008). However, increased scrutiny of their behavior in recent years has shown that multiscale models exhibit substantial improvements over conventional models in simulating the intermittency and intensity statistics of rainfall (DeMott et al. 2007). Improvements have been made with representing large-scale convectively coupled dynamical modes of atmospheric variability on a wide range of time scales, from interannual/El Niño (Stan et al. 2010) to subseasonal/Madden–Julian oscillation (Khairoutdinov et al. 2008; Benedict and Randall 2009) and diurnal (Khairoutdinov et al. 2005; Pritchard and Somerville 2009a,b; DeMott et al. 2007).

In a recent global analysis of the diurnal cycle of surface rainfall in a multiscale global model, we reported no evidence of propagating diurnal precipitation in the central United States, despite broad improvements in simulated diurnal variability overall (Pritchard and Somerville 2009a,b). In this previous work, the model was configured with a coarse horizontal spectral resolution at the exterior scale and 4-km cloud-system-resolving model horizontal resolution in the interior. At this early stage of multiscale modeling research it is not known whether the lack of propagating U.S. convective systems represents a tunable deficiency due to this particular model configuration, or a fundamental restriction of the physics admitted by the idealizations in the multiscale approach. The question is still open: is it possible for the multiscale global climate modeling approach to admit the physics of propagating diurnal convection in continental interiors?

This paper demonstrates that, indeed, under a slightly different configuration than was employed in Pritchard and Somerville (2009a,b), propagating central U.S. organized convection can be represented in a multiscale global model. Evidence of the signal emerges when the exterior model is upgraded to a finite-volume dynamical core at $1.9^\circ \times 2.5^\circ$ resolution and the embedded cloud-system-resolving model resolution is increased from 4 to 1 km. To investigate the realism of the propagating convective signal in this configuration, we analyze simulated storm propagation and genesis characteristics and explore the effect of the explicit convection approach on regionally relevant diurnal circulations and mean thermodynamics.

Section 2 describes the conventional and multiscale versions of the global climate model that are analyzed in this paper and their configuration. In section 3, the central U.S. diurnal convection signal is evaluated in the models, and the phase speed statistics of propagating events in the multiscale model are analyzed. In section 4, simulated thermodynamics and orographic diurnal circulations are compared in the model with and without the embedded explicit convection and evaluated against observations. In section 5, the simulated orogenesis mechanism, dynamical evolution, and multiscale structure of an individual organized propagation event is evaluated. In section 6, the simulated physics are discussed in light of established analytical theory, and a conceptual framework is developed to illustrate potential multigrid convective propagation pathways in the multiscale model.

2. Models, observations, and simulation design

Two heavily composited dynamically consistent best estimates of the observed atmospheric state, the Rapid

Update Cycle (RUC) operational data assimilation model and the European Centre for Medium-Range Weather Forecast (ECMWF) analyses, are used as a baseline for model evaluation.

The two climate models compared in this study are identical in every respect other than their treatment of subgrid convection and boundary layer effects. One is a standard global climate model, the National Center for Atmospheric Research (NCAR) Community Atmosphere Model (CAM). The other is a multiscale modeling framework (MMF), called superparameterized CAM (SP-CAM). In CAM, subgrid convection is handled diagnostically by statistical cumulus parameterizations and boundary layer schemes (Zhang and McFarlane 1995; Collins et al. 2004) whereas in SP-CAM these modules are replaced by an embedded, interactive, prognostic idealized cloud-system-resolving model.

The multiscale approach in SP-CAM is an interim strategy to better represent the physics of convection–climate interactions in a global model. This approach is several hundred times more costly to run than a conventional GCM but thousands of times less costly than a global cloud-system-resolving model. The approach works by resolving two discrete dynamical scale regimes: an exterior conventional global climate model and an interior cloud-system-resolving model (CRM). The multiscale approach is affordable via two key idealizations in the computationally expensive inner model. First, the amount of calculation is mitigated by undersampling in space (reduced dimensionality). Second, extra parallel communication overhead at the inner scale is avoided by splitting the embedded explicit models into thousands of laterally periodic subdomains. These isolated models can only interact via their mutual influence on the outer model's scale of dynamics. This allows multiscale models to scale efficiently on large, modern supercluster resources, of which conventional global models have been traditionally unable to take full advantage (Grabowski and Smolarkiewicz 1999; Khairoutdinov et al. 2005).

To ensure that the two resolved scales in a multiscale global model evolve consistently, and to evoke the appropriate convective response in the interior model, terms are added to the governing equations that relax the cloud model to the state of the outer model (Khairoutdinov et al. 2005). These terms nudge prognostic variables that the inner model shares with the outer model toward the large-scale resolved dynamical tendencies. Where such tendencies are convectively unstable, resolved convection produces a horizontal-mean state that stabilizes the outer model's thermodynamic state. This explicit ''convective adjustment'' feeds upscale as a ''superparameterization.'' Compared to conventional parameterization, this multiscale coupling approach has more degrees of freedom in the possible subgrid response to large-scale variations, which are inherited from the nonhydrostatic governing equations in the inner cloud-resolving model.

Previous publications documenting ''SP-CAM'' simulations have been based on an implementation of the Khairoutdinov and Randall cloud-system-resolving model (Khairoutdinov and Randall 2003) embedded in an older version of CAM3.0 that used a semi-Lagrangian global spectral dynamical core. Hereafter, we tag this original implementation SP-CAM3.0. In a recent analysis of the diurnal cycle of surface rainfall in SP-CAM3.0 at T42 horizontal truncation (approximately 350- to 700-km effective horizontal resolution) we found no evidence of propagating precipitation systems in the central United States (Pritchard and Somerville 2009a,b).

In this paper we analyze an updated version of SP-CAM in which essentially the same cloud-system model is embedded in a more recent development version of CAM (development software tag CAM3.5.32), which we hereafter call SP-CAM3.5. A key advantage of SP-CAM3.5 over SP-CAM3.0 is that the exterior model dynamics are formulated as a finite volume dynamical core, such that the subgrid response (including collective cloud-resolving model effects) is not smeared out by spectral dynamics. Furthermore, the conventional convection parameterization in CAM 3.0 was updated in CAM3.5 to include effects of convective momentum transport and dilution of convective plumes by increased entrainment.

SP-CAM3.5 and CAM3.5 are configured at $1.9° \times 2.5°$ horizontal resolution (approximately 230 km $\times$ 230 km at 40°N) with 30 vertical levels. In SP-CAM3.5 the inner cloud-system-resolving model domain is two-dimensional (height–longitude) on a vertical grid collocated with the outer model's interior 28 levels. The GCM time step (which is also the multiscale coupling interval) is 30 min.

As in prior MMF studies, the 2D cloud-resolving model momentum evolution is not transmitted upscale. It can be argued that this choice of approach is somewhat unsatisfactory. On this view, one may note that organized convection, notably a MCS, transports horizontal momentum countergradient (mean-flow acceleration) in certain atmospheric layers and downgradient (mean-flow deceleration) in other layers. Then the two-dimensional organized convective momentum transport, as formulated by Moncrieff (1992), is consistent with the quasi-linear geometry typical of an MCS. In support of this view, it can be pointed out that Kingsmill and Houze (1999) examined the momentum fields in all MCSs observed by airborne Doppler radar in the Tropical Ocean and Global Atmosphere Coupled Ocean–Atmosphere Response Experiment (TOGA COARE).

They showed that, even though MCSs in nature are three-dimensional, the fundamental properties of the Moncrieff model remain. Surely further research will be needed to settle this point conclusively and to establish all of the advantages and disadvantages of the choice of not allowing the embedded CRM to transmit momentum effects upscale in the MMF. At the present early state of development of MMFs, this and many other tentative model architecture decisions may need to be revisited in light of future experience.

We drive CAM3.5 and SP-CAM3.5 identically with a prescribed climatological sea surface temperature annual cycle and modern orbital and greenhouse gas parameters. The model runs freely, that is, no data assimilation is applied. Our simulations were initialized on 1 May, and we consider the first month a spinup period. Three months' output are analyzed [June–August (JJA)], which is sufficient to statistically characterize the key features of warm season central U.S. diurnal variability that distinguish the two models from each other and from observations.

3. Propagating diurnal convection

Figure 1 shows the classical ''reduced transect'' signature of propagating rainfall systems in the central United States in SP-CAM3.5. The time–longitude structure of the midtropospheric heating rate due to subgrid physics for CAM3.5 and SP-CAM3.5 (a model convection proxy) is compared against an independent observational convection proxy (IR brightness temperature at 11 μm observed from geosynchronous orbit during an arbitrary summer, 2005). In nature (Fig. 1a) convective phase lines are tilted, evidence of eastward diurnal convective propagation in the central United States. This observed propagation signal is modulated on synoptic time scales with consecutive packets of enhanced propagating diurnal convection occurring in intermittent episodes. While both models simulate intermittent periods of enhanced diurnal U.S. convection on synoptic time scales, only in SP-CAM3.5 are these episodes composed of consecutive, coherent, nocturnally persistent, diurnally propagating convective events. In SP-CAM3.5, convective phase lines are tilted but in CAM3.5 they are flat (Figs. 1b,c). The diurnal convection signal in CAM3.5 is sun-synchronous, short-lived, and does not propagate. The embedded explicit convection model in SP-CAM3.5 improved the space–time structure of the central U.S. diurnal convection cycle.

We derive the phase and propagation speeds of simulated organized convection in the lee of the Rockies in SP-CAM3.5 from analysis of the standard deviation of the physics package temperature tendency across

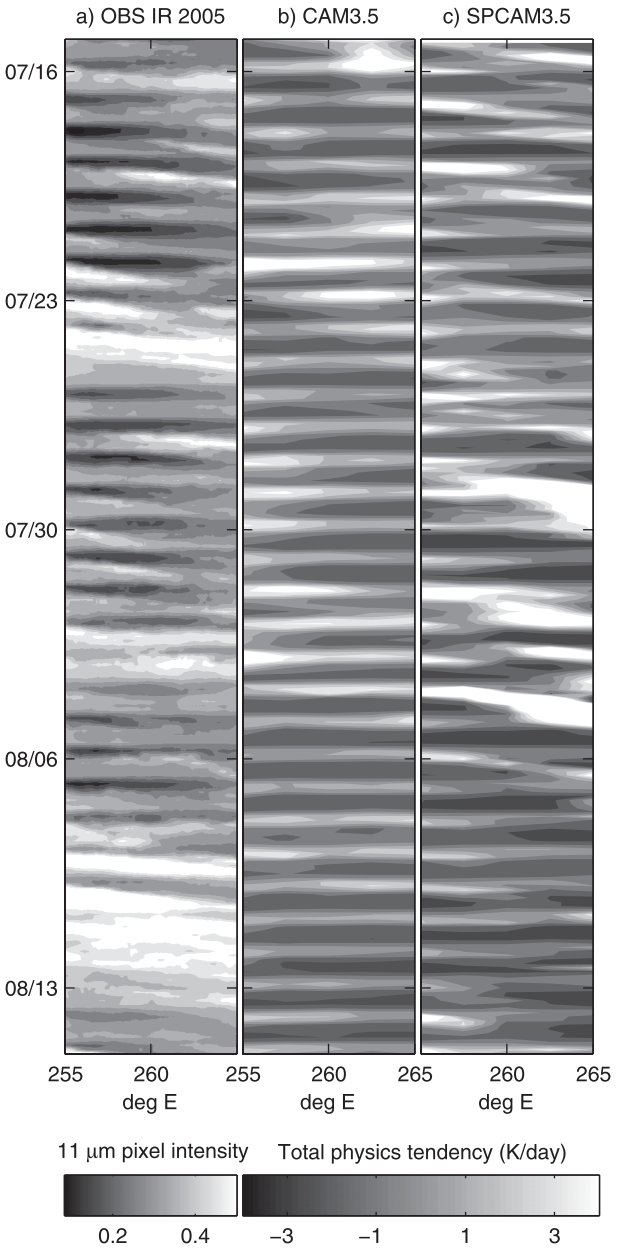

FIG. 1. Reduced transect comparison of the time–longitude structure of warm season diurnal convective activity in the lee of the Rocky Mountains between 35° and 45°N (a) as observed in 2005 from spaceborne infrared imagers and (b) as diagnosed from the total physics package temperature tendency averaged between 350 and 750 hPa in the free-running CAM3.5, and (c) in SP-CAM3.5 simulations.

tropospheric model levels (hereafter called ζ). Due to the characteristically intense vertical dipole heating-atop-cooling structure of these organized convective systems (see section 6), ζ is a convenient model proxy for the simulated storm location. Long-lived propagating convective systems in a sheared environment are a

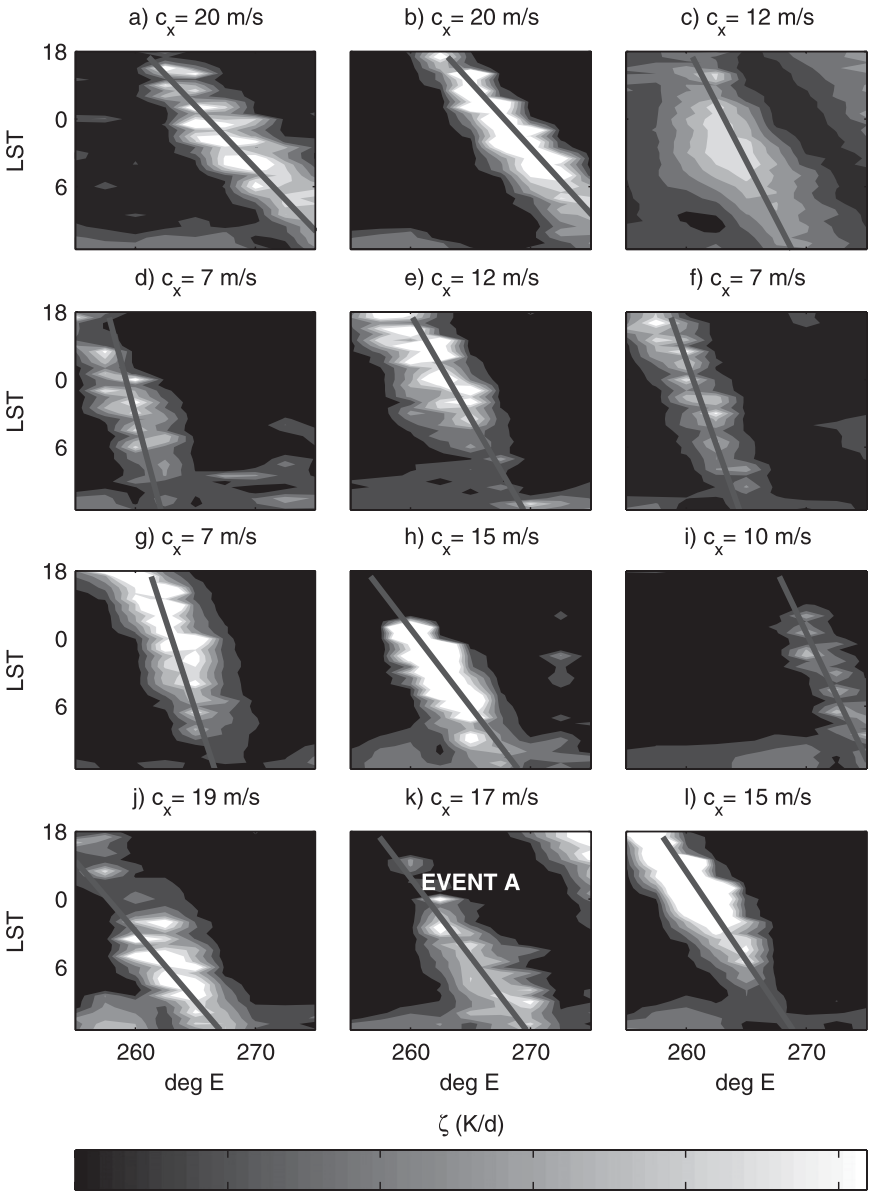

FIG. 2. Time–longitude section showing the standard deviation across tropospheric model levels of the physics package temperature tendency (a storm location proxy) and fitted zonal phase speed (overlaid line) for 12 of 13 propagating convective events simulated by SP-CAM3.5 in the lee of the Rockies.

product of interaction between environmental shear and dipole-like latent heating, formed by latent heat released in mesoscale slantwise ascent and the evaporation of precipitation in mesoscale descent as described in the review paper of Moncrieff (2010).

Figure 2 shows Hovmöller maps of ζ for each simulated nocturnal storm in SP-CAM3.5 at the latitude of its maximum convective heating. The zonal phase speed c_x (slope of white line) was estimated for each propagation event by numerically fitting a phase line segment Gaussian envelope function of the form

$$F(x,t) = \exp[(x - x_0 - c_x t)^2/\sigma],$$

where $\sigma \approx 65$ km and (x_0, c_x) were constrained using Monte Carlo variation and optimal pattern correlation of the assumed form F. This approach is similar to that applied in Matsui et al. (2010).

Figure 3a shows that the ensemble of simulated orogenic convective events in SP-CAM3.5 travels eastward at speeds in the range of 7–20 m s^{-1}. Reassuringly, this is within the range of the observed zonal speed of orogenic mesoscale convective systems in the lee of the Rockies, determined from radar reflectivity data to range from 7 to 30 m s^{-1} (Carbone et al. 2002).

In nature the travel speed of mesoscale convective systems involves both an advective and a propagating component; that is, the systems are not simply advected by the mass- and/or buoyancy-weighted mean tropospheric flow (Carbone et al. 2002; Moncrieff 1981). The zonal *propagation* speed, $c_x - \overline{u}$, of the simulated orogenic convective events in SP-CAM3.5 was determined by subtracting the mass-weighted mean tropospheric zonal wind $\overline{u} = \int_{p_0}^{p_{\mathrm{TTL}}} u\,dp / \int_{p_0}^{p_{\mathrm{TTL}}} dp$ from the zonal speed, where u was averaged horizontally in space and in time along the lines overlaid in Fig. 2.

Figure 3b shows a histogram of $c_x - \overline{u}$. Most of the simulated convective systems exhibit a zonal propagation in excess of 2 m s^{-1} relative to the tropospheric background flow, typically propagating in the direction of the ambient westerlies. As in Carbone et al. (2002), the median implied steering level (height at which the travel speed equals the environmental flow) for the simulated events is in the range of 400–500 hPa (Fig. 3c).

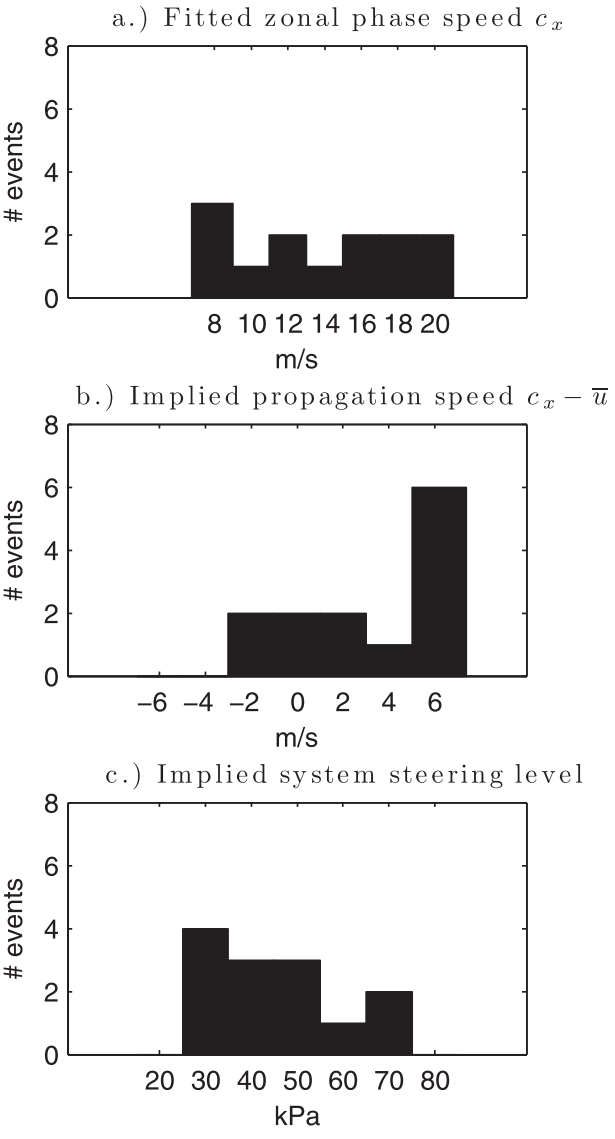

FIG. 3. Histograms across the ensemble of simulated propagating convection events showing (a) the distribution of c_x, the fitted zonal phase speed from Fig. 2, (b) the implied storm propagation speed relative to the mean mass- weighted background flow, $c_x - \overline{u}$, and (c) the implied storm steering level.

4. Regional flows, thermodynamics, and synoptics

Observations indicate that episodes of orogenic propagating diurnal convection in the lee of the Rockies are associated with conditions of synoptic uplift, zonal geostrophic flow aloft, low-level shear, and higher than usual regional water vapor content (e.g., Maddox 1983; Laing and Fritsch 2000; Jirak and Cotton 2007). Carbone and Tuttle (2008) describe how two aspects of the composite regional diurnal dynamics in the lee of the Rockies—the Great Plains low-level jet (LLJ) and mountain–plains solenoid (MPS)—''conspire'' to promote a dynamical environment conducive to the upscale development and nocturnal enhancement of propagating convective systems initiated upstream over the Continental Divide. In this section, we evaluate these thermodynamic and dynamic aspects of CAM and SP-CAM behavior against baseline RUC analyses.

Figure 4 contrasts the climatological warm season thermodynamic state in the two global models against the RUC observational analysis over the central United States. In CAM3.5 the warm season atmosphere is too dry (precipitable water bias ranging from −2 to −10 mm). In SP-CAM3.5, there is more moisture available to feed convection (+2 to +4 mm). It is conceivable that the propagating convective signal in SP-CAM3.5 is related to this improvement in summertime U.S. climate. But offline sensitivity tests rule this out: even when constrained to follow the SP-CAM3.5 climate trajectory on interdiurnal time scales, CAM3.5 does not admit a propagating convective signal (not shown).

Figure 5 contrasts the upward branch of the simulated composite mountain–plains solenoidal circulation in CAM3.5 and SP-CAM3.5 with the baseline representation in the operational RUC data assimilation model. As described in Carbone and Tuttle (2008), the thermally driven nocturnal reversal of the solenoid—from

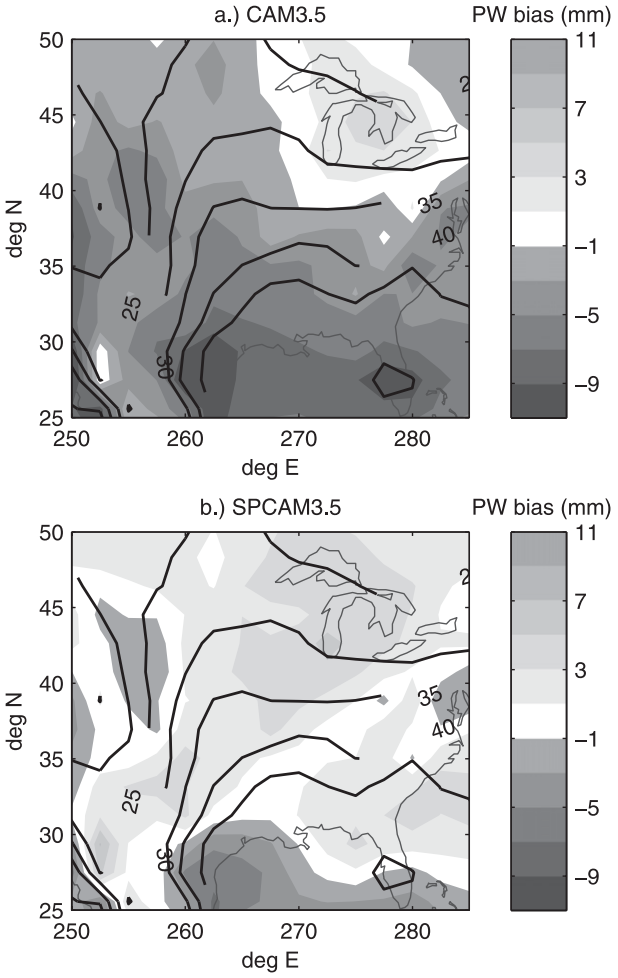

FIG. 4. JJA climatological precipitable water anomaly at 0000 UTC (shading, mm) for the single-season (a) SP-CAM3.5 and (b) CAM3.5 simulations, relative to the RUC 2003 analysis (contours, interval = 5 mm).

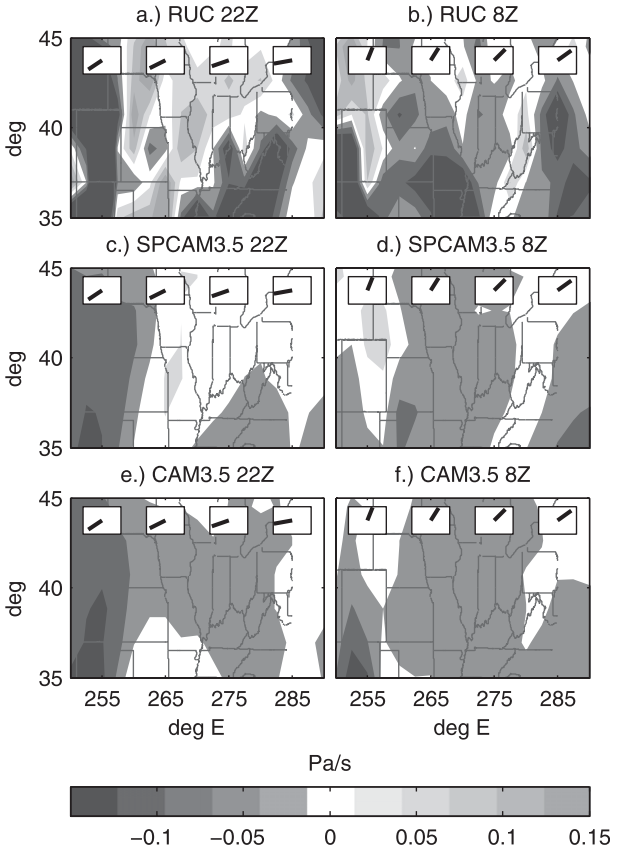

FIG. 5. Three-hour average vertical pressure velocity centered at (a),(c),(e) 2200 and (b),(d),(e) 0800 UTC comparing the upward branch of the central U.S. solenoidal diurnal mountain-plains circulation in (a),(b) the RUC analysis during JJA 2003 to JJA averages of the single-season (c),(d) SP-CAM3.5 and (e),(f) CAM3.5 simulations. Local time of day is depicted on 24-h clock icons.

daytime conditions of strong ascent during the day over the Continental Divide and broad subsidence over the Central Plains (Fig. 5a) to strong descent over the Continental Divide and weak ascent over the Plains (Fig. 5b)—corresponds to a plains uplift environment favorable for sustaining nocturnal mesoscale convective systems. The western, upward branch of the solenoidal circulation is only weakly simulated by both climate models, perhaps due to the coarse model resolution (smooth low orography) inhibiting local topographically driven convection associated with this uplift regime (Lee et al. 2008). However, the nonlocal daytime plains descent phase of the MPS is better represented in SP-CAM3.5 (cf. Figs. 5c and 5e). A similar nonlocal improvement occurs in SP-CAM3.5 in a descending circulation adjacent to the Appalachian mountain chain.

In nature the descent phase of the mountain–plains solenoid produces a subsidence inversion (barrier to convective ascent) over the Great Plains, which traps daytime surface buoyancy over a vast area (Carbone and Tuttle 2008). As a result, the CAPE generated by daytime surface heating accumulates and is focused into a narrow leeside zone by easterly upslope surface density flows (Dirks 1969; Tripoli and Cotton 1989, hereafter TC89). Mountain-generated cumulonimbus advecting off the Rockies can tap into this concentrated potential buoyancy reservoir, which in the presence of deep zonal shear can produce rapid upscale growth into mesoscale convection systems (TC89). Figure 6 shows that the strength of the capping inversion is too weak in CAM3.5, but is strengthened using the embedded explicit convection approach in SP-CAM3.5. This is consistent with the SP-CAM3.5 improved representation of the daytime descent phase of the solenoidal circulation discussed above

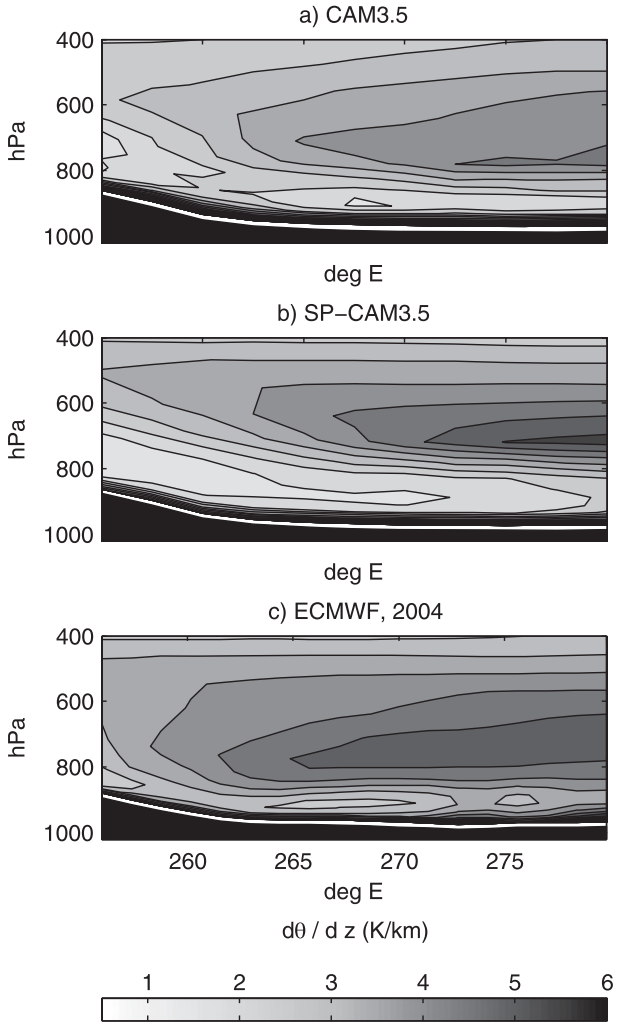

FIG. 6. Pressure–longitude section showing JJA climatological static stability $\partial\theta/\partial z$ averaged from 35° to 45°N in the lee of the Rockies for (a) CAM3.5, (b) SP-CAM3.5, and (c) a year of ECMWF interim reanalysis. Surface topography is shown in black.

and suggests that SP-CAM3.5 more readily concentrates accumulated plains CAPE in the leeside convergence zone.

The northern terminus and eastern flanks of the low-level jet circulation are important sources of localized low-level nocturnal moisture convergence, temperature advection, and low-level vertical shear, which help sustain organized convective systems into the night along distinct latitude ''corridors'' (Tuttle and Davis 2006; Trier et al. 2006; Jirak and Cotton 2007; Trier et al. 2010). Figure 7 evaluates the warm season composite nocturnal evolution of the 850-hPa moisture convergence zones associated with the low-level jet circulation in the two models against diurnally composited RUC data. The analyses show a broad zone of moisture convergence from 38° to 45°N, 265° to 270°E, which intensifies from 2200 (0500) to 0400 (1100) local time (UTC) (Figs. 7a–c), tracking the northeastern terminus of the evolving low-level jet circulation as it veers increasingly eastward throughout the night. Dual local vapor convergence maxima emerge in the early morning hours of the composite RUC data, centered at 32°–34°N, 262°E and 38°–40°N, 270°E (Fig. 7c). The northernmost of these maxima has previously been linked to a corridor of preferred MCS propagation at 40°N (Tuttle and Davis 2006).

Like most coarse-resolution climate models, the resolved physics of SP-CAM3.5 and CAM3.5 admit the essential ingredients for thermally driven orographic low-level jet dynamics (Ghan et al. 1996). However, the chronology and structure of the associated 850-hPa moisture convergence zones are different in the two models. In CAM3.5 there is only a single broad zone of nocturnal maximum convergence in the nocturnal composite (Figs. 7d–f). In contrast, SP-CAM3.5 exhibits a dual maximum nocturnal moisture convergence structure, as in the data (Figs. 7g–i). In SP-CAM3.5, LLJ vapor transport and the northern convergence maximum extend farther north than in CAM3.5 and observations. The preferred latitude of orogenic convective complexes in SP-CAM3.5 coincides with the northernmost moisture convergence maximum at 45°N.

Figure 8 contrasts the shear characteristics of the low-level jet circulation in the observations and models. Wind shear below 3 km is an important organizing influence for MCS generation in nature and is modulated diurnally by the low-level jet. In the RUC data, maximum anomalous low-level shear occurs near local midnight (0700 UTC) in a compact zone between 30° and 40°N and weakens into the morning. Both climate models reproduce this aspect of the LLJ, but in SP-CAM3.5 the zone of enhanced nocturnal shear extends farther north, to almost 50°N. Although low-level shear cannot influence convection by design of the cumulus parameterization in CAM3.5 (except through convective momentum transport, which reduces the shear), its zonal component is an organizing influence on 2D convection in the embedded cloud resolving model arrays in SP-CAM3.5.

Reassuringly, synoptic conditions similar to those observed in nature accompany simulated propagating diurnal convection events in SP-CAM3.5. Figure 9 shows the anomalous (with respect to warm season model climatology) sea level pressure, precipitable water, and vertically integrated water vapor transport, $q\mathbf{V}$, for 12 propagation episodes that took place during the single-summer SP-CAM3.5 simulation. Most of the propagation events occur during periods of synoptic uplift (anomalously low surface pressure) in the lee of the Rockies (Figs. 9a,b,d,e,g,h,j). The remaining events occur during conditions of anomalously high precipitable water (Figs.

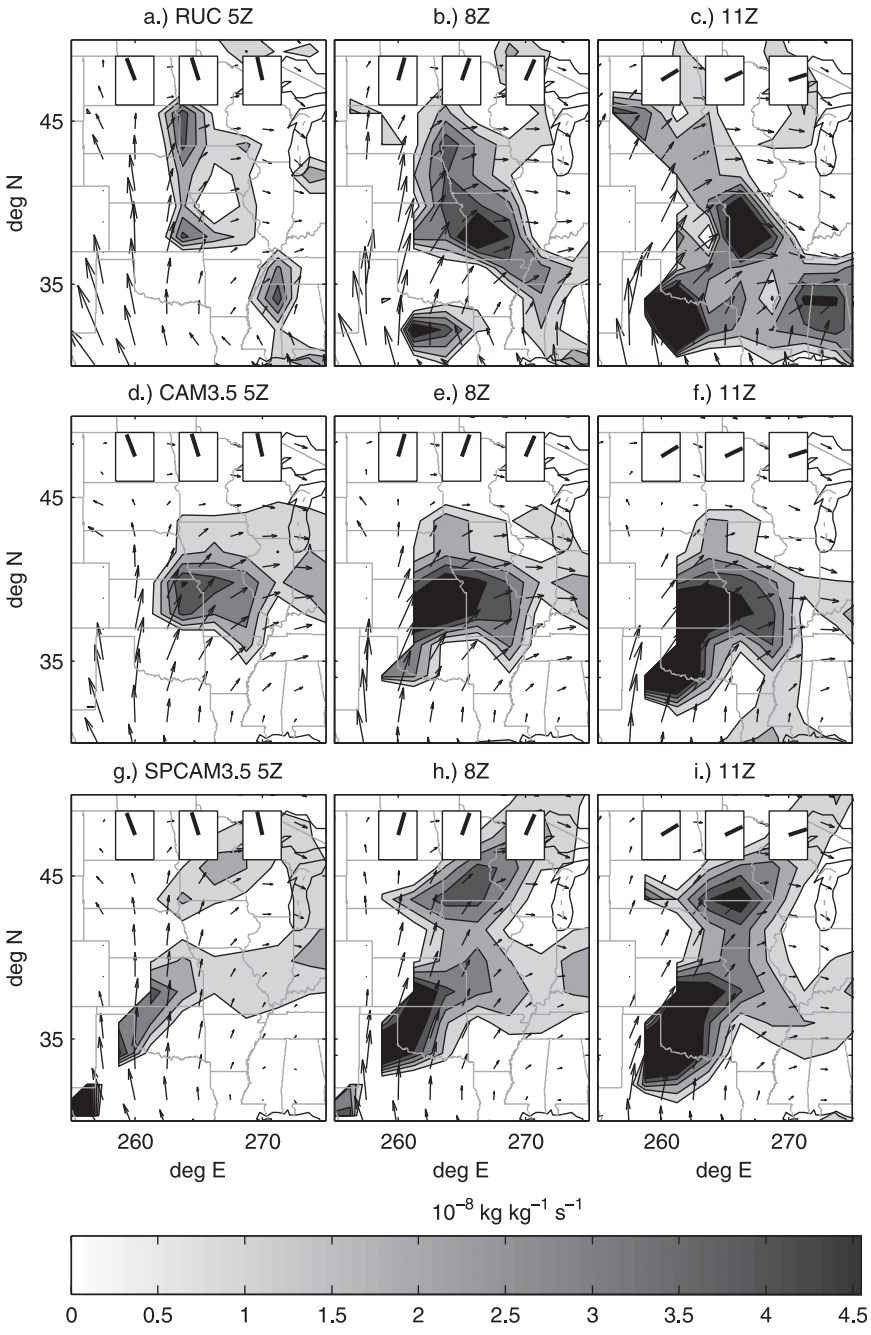

FIG. 7. Maps over the central United States comparing the nocturnal evolution of the 850-hPa vapor transport (vector field; $q\mathbf{V}_H$) showing the Great Plains LLJ and its associated moisture convergence [shading; $\mathbf{V} \cdot (q\mathbf{V}_H)$] in (a)–(c) the 2003 RUC analysis, compared to global simulations using (d)–(f) CAM3.5 and (g)–(i) SP-CAM3.5.

9c,f,i,k,l). The signature of a southerly jet structure in the anomalous water vapor transport vector field for several events (Figs. 9d,e,f,g,j,k,l) further suggests that enhanced moisture convergence and wind shear due to low-level jet flow into the Great Plains also plays a role in generating organized propagating nocturnal convection in SP-CAM3.5.

5. Genesis and multiscale structure of a propagating event

We now focus on a specific simulated propagation event (hereafter event A; the topmost tilted phase band in Fig. 1c) for additional physical process analysis. Event A was chosen for in-depth analysis because the weather

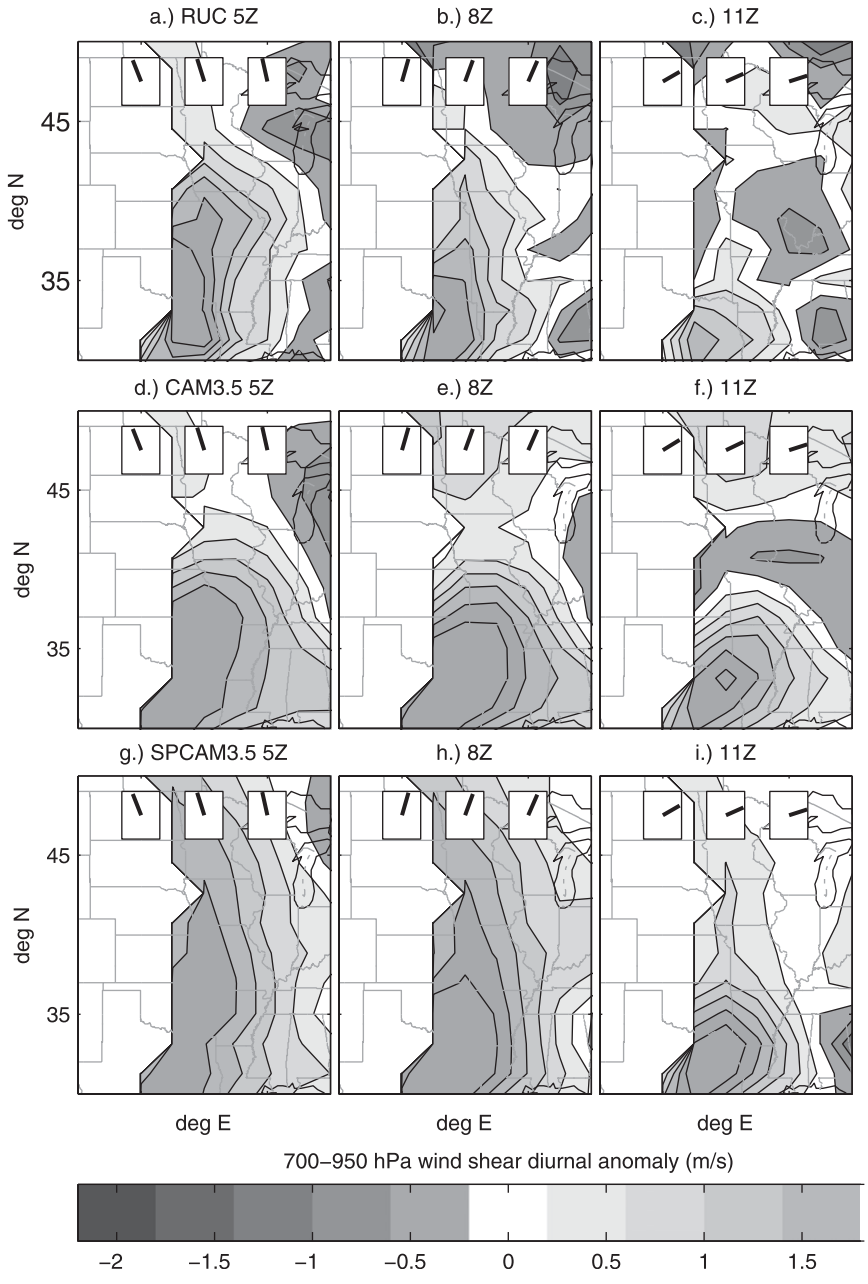

FIG. 8. As in Fig. 7, but showing the diurnal anomaly of low-level wind shear magnitude (700 − 950 hPa) associated with the Great Plains LLJ in (top) the 2003 RUC analysis, (middle) CAM3.5, and (bottom) SP-CAM3.5.

state in SP-CAM3.5 over the central United States was dominated by abnormally zonal geostrophic flow aloft, due to the positioning of a synoptic long-wave pattern (Fig. 10). This is an ideal environment to test the model's unsteady orogenesis mechanism against a classical conceptual dynamical model developed by TC89 around a historical case study of observed mesoscale convective system orogenesis that took place in a similar weather state.

Figure 11 shows the evolution of condensate and large-scale horizontal winds during event A. Initially (Fig. 6a) two condensate structures (contours) are visible. The westernmost is event A near 250°E, an organized convective system that has just begun to form. The easternmost (270°E) is a mature convective system that was generated 24 h prior near 250°E, but has since traveled 20° (1700 km) to the east at approximately 20 m s^{-1}. The formation of event A occurs during

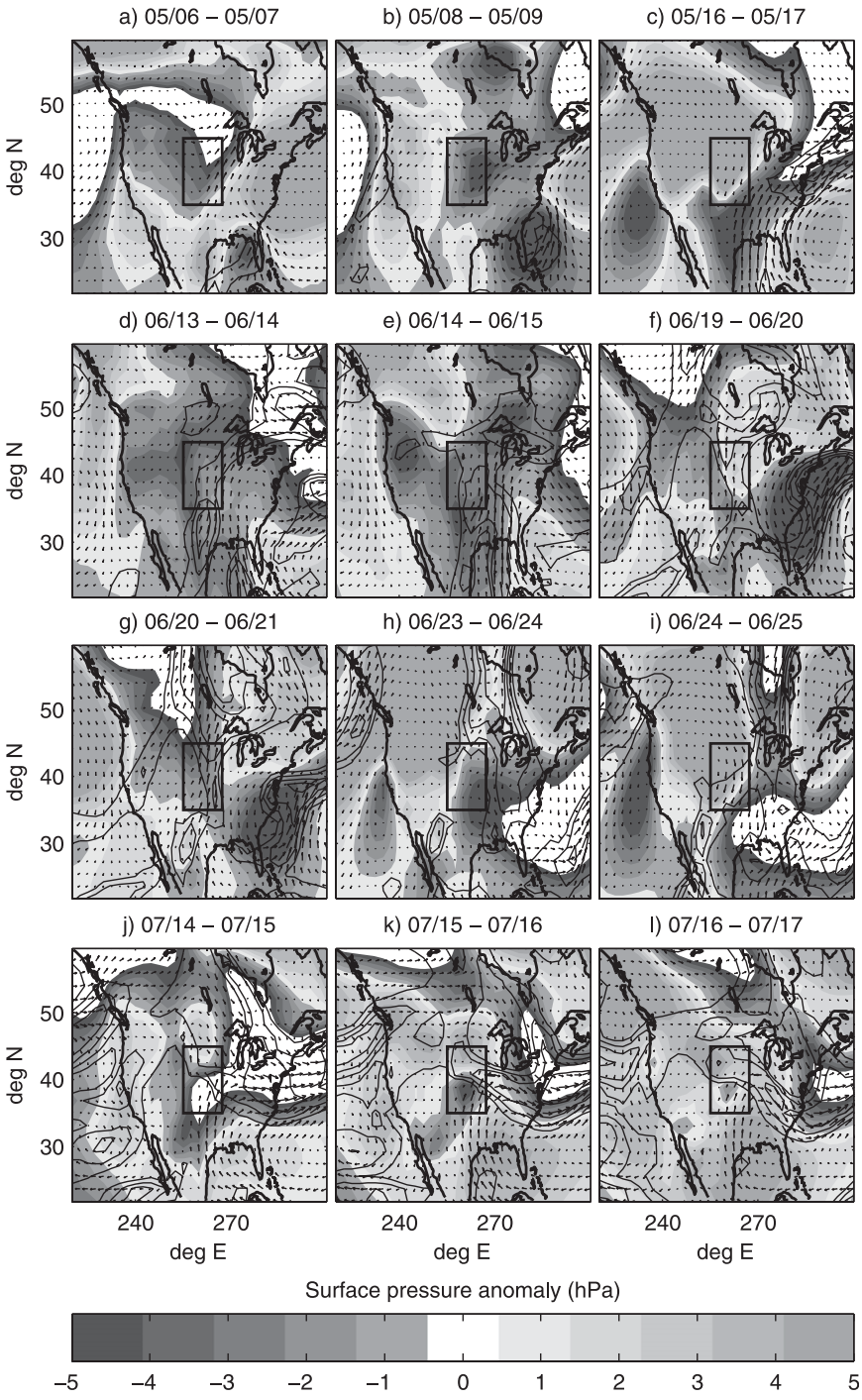

FIG. 9. Composite anomaly maps over the central United States showing the deviation of surface pressure (shading, hPa), positive column water vapor mass anomalies (contour interval = 4 g m^{-2}), and column water vapor transport (vector field) during 12 propagating convection events in SP-CAM3.5, relative to its simulated seasonal JJA climatology.

conditions in which the zonal westerlies are deeply sheared and a shallow easterly upslope surface wind layer converges near 260°E (Figs. 6a,c,e,g). As in the TC89 model, condensate is first produced by locally forced deep mountain convection at 2030 UTC (Figs. 6a,b; contours). Upscale development occurs around 0000 UTC when the system reaches the leeside convergence zone (Fig. 6c.). Convection weakens at 0430 UTC and reintensifies by

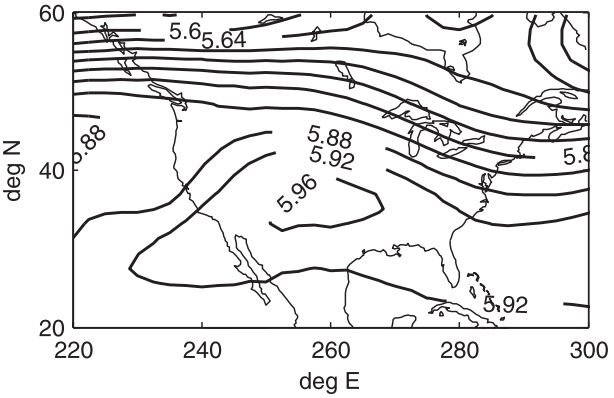

FIG. 10. SP-CAM3.5 500-hPa geopotential height (km) showing the synoptic state during a simulated 3-day packet of consecutive diurnal orogenic convection propagation.

1130 UTC when it coincides with the LLJ inflow. A northerly wind component near 500 hPa develops along the western flank of the organized convective system, suggesting flow balance on the large-scale grid. Such balance is clearly evident for the mature organized convective system generated the previous day (Figs. 11b,d,f), which exhibits a classical stacked cyclone–anticyclone signature.

Figure 12 shows the vertical velocity and stability during the same period. At 2030 UTC, the plains inversion traps locally generated surface instability in a thin boundary layer. To the west the cloud-topped afternoon boundary layer is deep. The leeside convergence zone causes upward motion near 260°E (Fig. 12a). This plume supplies zonally converged, inversion-trapped plains instability upward and feeds convection expansion. Convective heating aloft is straddled by mesoscale downdrafts (Fig. 12e; 255°E, 270°E at 300 hPa). In the mature phase, deep vertical velocity associated with convective heating produces local breaks in the capping inversion (Figs. 12c,d; 275°E at 800 hPa).

Figure 13 visualizes both resolved grids in SP-CAM3.5 simultaneously during the propagation event on the day before event A, showing evidence of multigrid convection–dynamics interactions across the two resolved scales. Propagating 3D condensate metastructures transcend individual embedded explicit convection subdomains but exhibit morphology on larger scales reminiscent of observed mesoscale convective systems (deep precipitating system ''core,'' leading ice/virga anvil). The condensate structure of the embedded cloud-resolving model states show distinct organization resulting from 2D shear and cold pool effects. That the system coherently propagates across many embedded cloud model subdomains while retaining its metastructure emphasizes interaction between the two resolved physical scales.

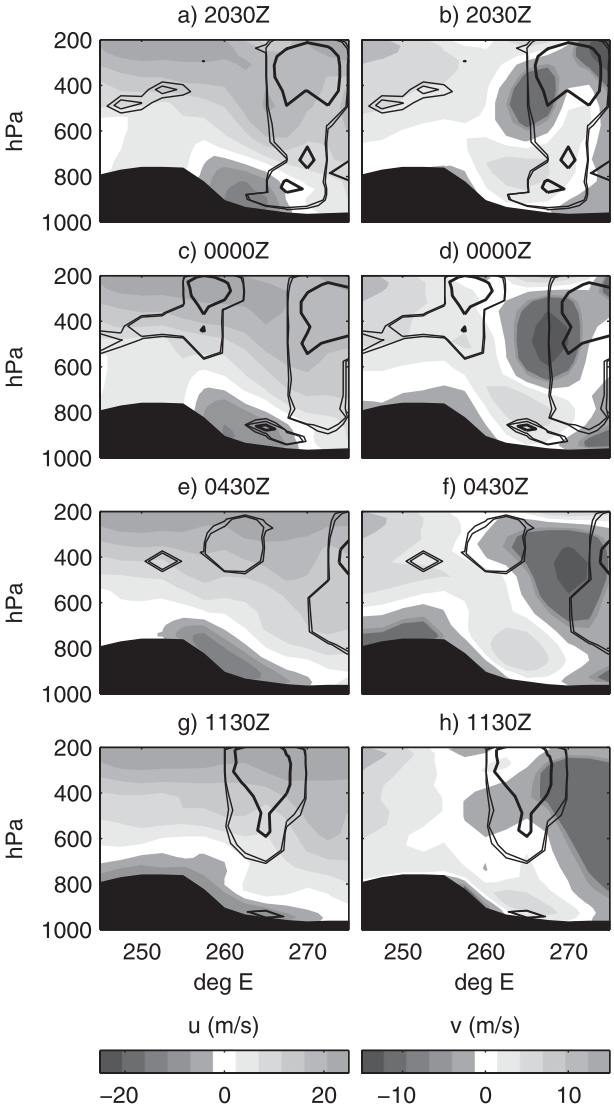

FIG. 11. Height–longitude structure at 40°N showing the time evolution of (left) zonal and (right) meridional wind during event A. Condensate concentration contours are superimposed for values of (0.005, 0.01, 0.1, 1) g kg^{-1}.

6. Discussion

a. Dynamical considerations

Theoretical investigations have shown that as well as the CAPE normally associated with deep convection, the highly organized mesoscale convective system (MCS) is partly sustained by the mean-flow kinetic energy and the work done by the horizontal pressure gradient. These dynamical forms of energy are fundamental to the convective organization process and the interaction of environmental shear with latent heating atop evaporative cooling [see review by Moncrieff (2010)]. This dipole-like heating projects onto the first-baroclinic

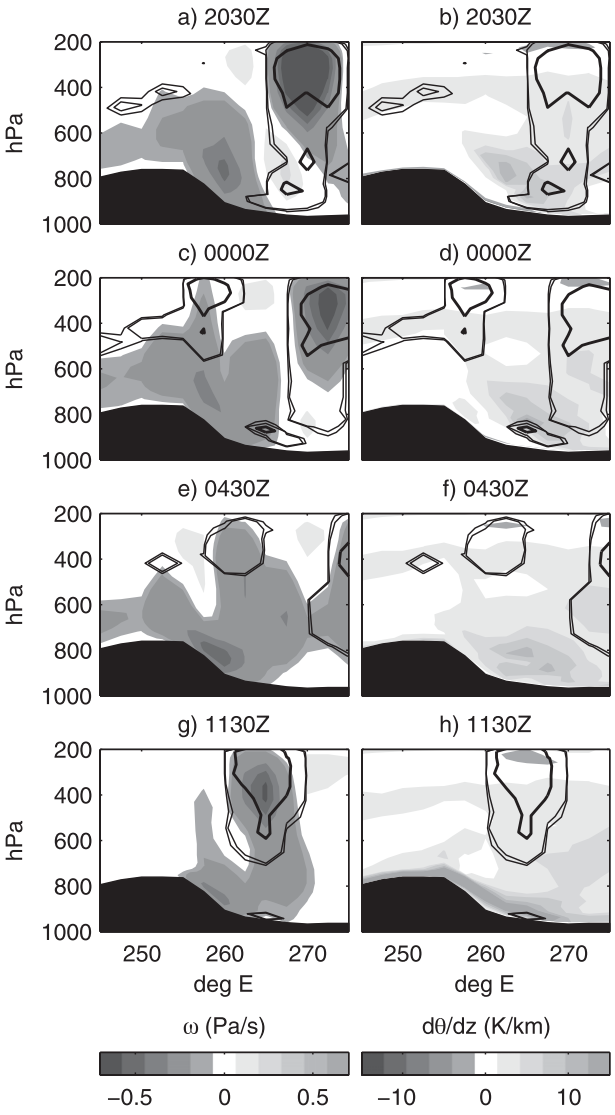

FIG. 12. As in Fig. 11 but for (left) vertical pressure velocity and (right) $d\theta/dz$.

gravity wave mode and is important for injecting kinetic energy upscale (Pandya and Durran 1996; Moncrieff and Liu 2006; Correia et al. 2008). The mesoscale circulations occur as distinctive regimes of organized airflow (Moncrieff 1981). The simplest possible (i.e., archetypal) dynamical model distinguishes the following regimes of slantwise MCS-type convective overturning: (i) a purely propagating system in which the relative inflow derives entirely from ahead of the system, (ii) a symmetric system in which the updraft and downdraft have comparable depth, and (iii) a system that contains hydraulic-jump-like ascent in the cooling region (see Fig. 2 of Moncrieff 1992). These three regimes are distinguished by a measure of dynamical efficiency, that is, the quotient of the work done by the horizontal pressure gradient and the kinetic energy available from shear. None of these slantwise circulations is present in CAM (or any standard climate model) because first, traditional convective parameterizations do not represent the salient dynamics of convective organization and second, the horizontal resolution of the model is insufficient to explicitly simulate these circulations.

We have already shown that organized circulations occur in SP-CAM3.5. A salient question concerns their realism. Figure 14 shows the dipole-like heating for a dozen propagating events in SP-CAM3.5 and the zonal component of airflow relative to the traveling systems; that is, $(u', \omega) = (u - c_x, \omega)$. In most of the events a distinctive overturning solenoidal circulation exists ahead of the system (e.g., Fig. 14g, rotational relative circulation centered near 270°E and 500 hPa), in broad agreement with TC89. However, the depth of the surface easterly inflow is unusually deep, ranging from 4 to 7 km (Figs. 14b,e,k,l). A prevalent feature of this inflow is the up–down circulation that traverses the system front to rear, sometimes featuring deep vertical displacement (e.g., Figs. 14b,k), consistent with the above archetypal hydraulic jump regime. This regime contrasts with orogenic propagating MCSs over the continental United States simulated by Moncrieff and Liu (2006) and Trier et al. (2006) and verified against a continental-scale radar network. Those simulations are consistent with the symmetric archetypal regime. It is not understood why the SP-CAM3.5 convective systems tend to have a prevalent jumplike morphology. Among possible explanations is that evaporative cooling (associated with the cloud-microphysical parameterization in the embedded explicit convection with emphasis on the stratiform region and mesoscale downdrafts) is too strong. In summary, the morphology of the airflow organization simulated by SP-CAM3.5 differs from the natural world, and also from cloud-system simulations (e.g., Grabowski and Moncrieff 2001) and the above dynamical efficiency with emphasis on the simulated horizontal pressure gradient. A basic study of these important aspects while necessary is beyond the scope of this present paper.

b. *Role of dipole heating in shear flow compared to cold-pool triggering*

It was argued above that the basic reason why SP-CAM3.5 generates organized propagating convection is that the embedded cloud-system-resolving models produce the dipole heating required for mesoscale convective organization in shear flow. The upper-tropospheric latent heating overlies a deep evaporative cooling layer that typically extends from the surface to 600 hPa in the model. As explained above, the dipole-like diabatic

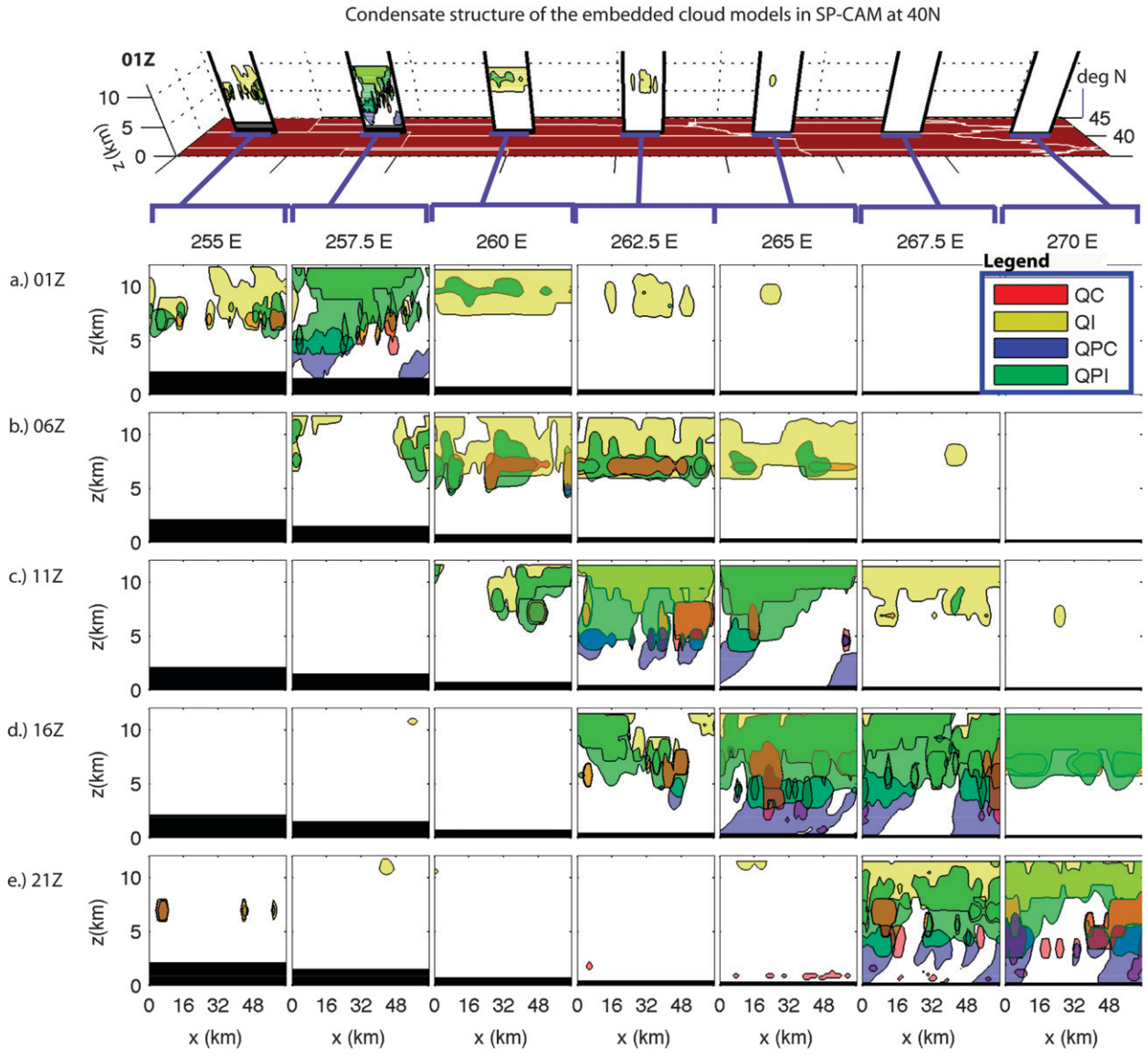

FIG. 13. Time–longitude matrix of height–longitude sections showing snapshots of condensate within adjacent cloud resolving models at 40°N in SP-CAM3.5 during a simulated organized propagation episode, at 5-h intervals from (a) to (e). Shaded transparent contours outline the 0.01 g kg^{-1} threshold for nonprecipitating cloud water (red, QC), nonprecipitating cloud ice (yellow, QI), precipitating cloud water (blue, QPC), and precipitating cloud ice (green, QPI) within the embedded explicit convection model subdomains shown above. Surface orography is shown in black.

heating is linked to the propagation physics of MCS in shear flow *on the coarse SP-CAM3.5 outer grid*. The convective heating profiles associated with the mesoscale convective systems project favorably onto first-baroclinic gravity wave modes. Such a slow-manifold control of the propagating systems in SP-CAM3.5 is evidenced by the dynamical balance in Fig. 11. This property is consistent with the convectively generated potential vorticity propagation mechanism of Raymond and Jiang (1990) and Li and Smith (2010). Indeed, convectively generated diurnal potential vorticity anomalies are routinely spawned by the organized convective events in SP-CAM3.5 (not shown).

On the other hand, cold pools in the form of density currents generated by convective downdrafts impinging on the underlying surface and/or convectively generated gravity waves have an important local effect on the *finescale cloud-system-resolving grid*. The density currents continually trigger fresh cumulonimbus, which, in a sheared environment, organize upscale into mesoscale convective systems (e.g., Thorpe et al. 1980; Rotunno et al. 1988; Lafore and Moncrieff 1989). However, contrary

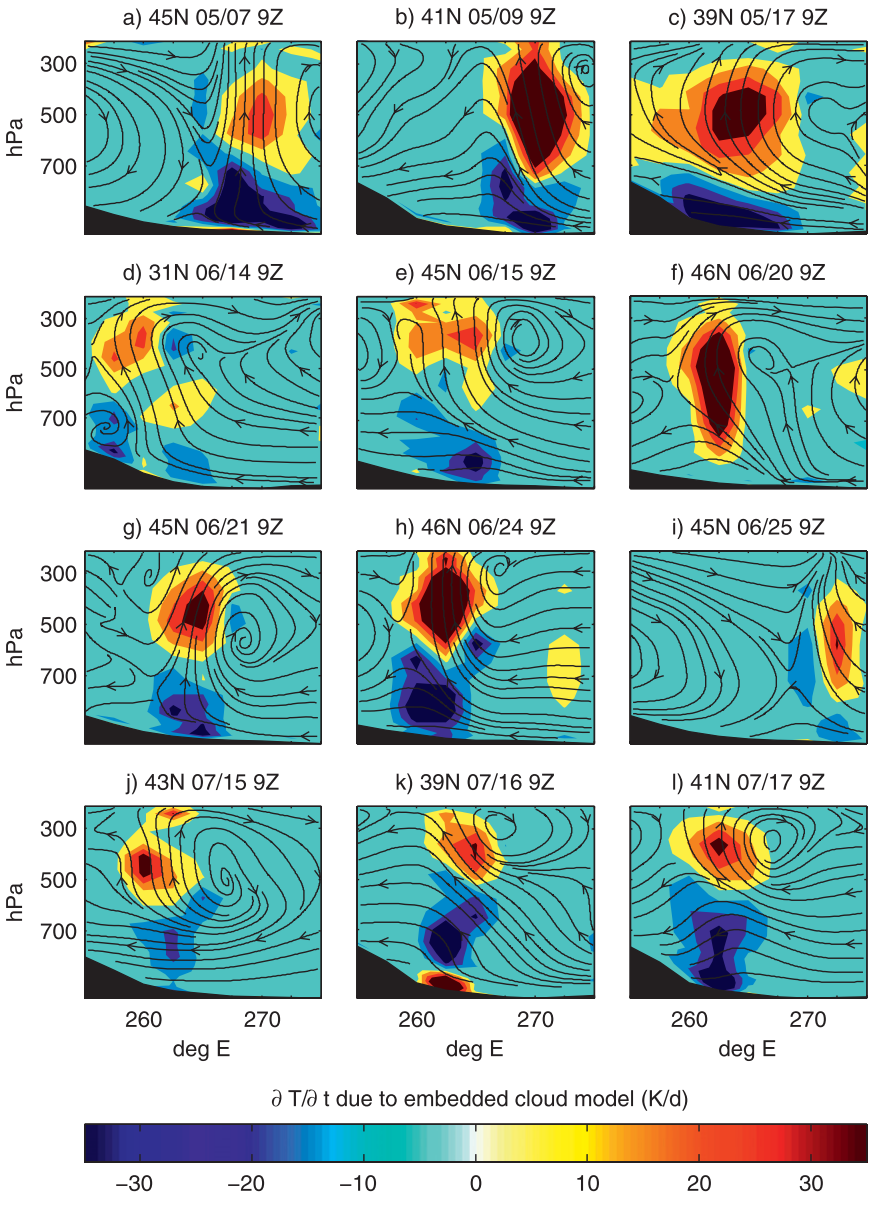

FIG. 14. Pressure–longitude sections at 0200 local time, showing storm-relative zonal flow (solid streamlines) atop the convective heating structure (temperature tendency due to the embedded CRM; thin contours at 10 K day^{-1} increments, negative contours dotted; light shading for $\partial T/\partial t > +15$ K day^{-1}, dark shading for $\partial T/\partial t < -15$ K day^{-1}) for 12 separate instances of MCS propagation in the lee of the Rockies in SP-CAM3.5.

to the implications of Carbone et al. (2002), Carbone and Tuttle (2008), and others, neither cold pools nor gravity waves can explain the propagating MCS simulated by SP-CAM3.5. The periodic lateral boundary conditions imposed on the cloud-system-resolving model, a key aspect of the MMF approach that makes it scalable for massively parallel climate modeling, trap the density currents within each finescale domain, hence precluding long-range interaction on the coarse grid.

c. *Multigrid propagation of organized convection across scales*

Figure 15 is a framework for how convective signals can propagate over many GCM grid boxes in a multiscale model despite the restriction of lateral periodicity in the embedded cloud-system-resolving models. Consider a thought experiment in which 1) the resolved tendency in the outer, large scale (LS), model of SP-CAM

has just produced organized convection in the embedded explicit convection model at horizontal location x_1. Consequently, 2) the CRM induces a convective heating typical of organized convection (i.e., containing a deep stratiform cooling layer) onto the LS model at x_1. This subgrid diabatic forcing projects onto first-baroclinic LS waves such that, on the following LS time step, 3) resolved convection information at x_1 propagates, as mediated by resolved LS wave dynamics, to an adjacent horizontal location x_2. The LS model at x_2 4) transmits received wave-induced perturbations of temperature, momentum, and shear to its embedded CRM via the nudging terms that link the LS to the CRM. Provided the CRM at x_2 is initially in a state that is susceptible to convecting in response to such perturbations, nonlocal convection propagation can occur despite the fact that the CRMs are isolated and periodic. The limiting time scale for the communication of convective information between the two scales is the large-scale model time step. When it is less than the lifetime of individual cumulus elements or organized 2D cumulus systems, as in the simulation here (30 min), stages of the horizontal mean plume life cycle in the CRM can interact with dynamical modes resolved by the large-scale model.

Figure 16 shows how the scale interface in SP-CAM3.5 was redesigned via the embedded explicit convection approach, emphasizing the introduction of subgrid memory. The inclusion of a *prognostic convective system life cycle* is a crucial extra degree of freedom that allows subgrid heating profiles in SP-CAM3.5 to respond to organizing environmental influences such as wind shear or convectively generated organized flows. In CAM3.5, subgrid convective heating is slave to the resolved dynamical tendency of a single instability metric accumulated during a single GCM time step. On the other hand, in SP-CAM3.5 resolved tendencies of temperature, water, momentum, and condensate are instead applied as a forcing on a prognostic embedded explicit convection integration. The consequent heating profile adjustment is determined by the cloud-system-resolving model under this forcing. Being an integration rather than a diagnostic calculation, the explicit cloud-system-resolving model physics is, in part, determined by the initial conditions. In other words, memory exists at the smallest resolved scale in the multiscale modeling framework. As such, if instability is generated by large-scale temperature and moisture advection and shear, the CRM will tend to develop organized convection, that is, propagating mesoscale convective systems. In a separate context, organization memory was recently introduced in the subgrid convection package of a conventional global model in Mapes and

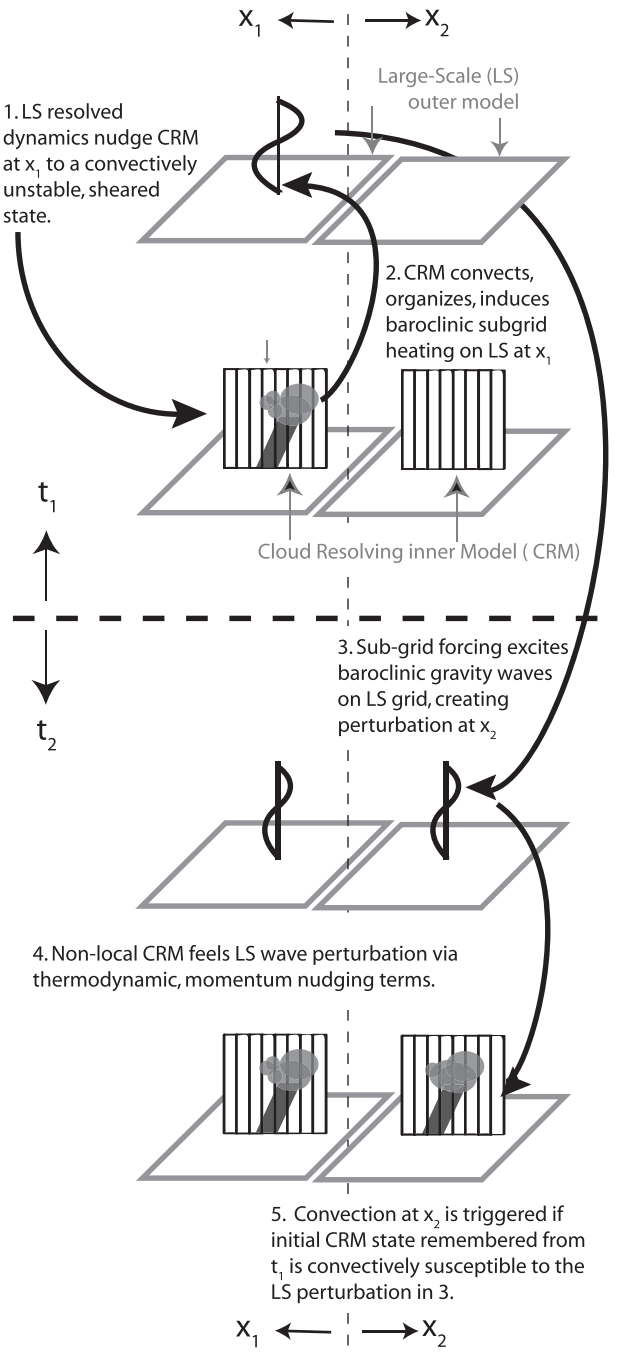

FIG. 15. Conceptual schematic illustrating how multigrid propagation of convective signals can occur across the two resolved scales—(top) interior cloud-resolving model (CRM) and (bottom) exterior large scale (LS)—contained in SP-CAM3.5. A sequence of events is shown at adjacent LS grid columns (left) x_1 and (right) x_2, straddling the transition from (above dashed line) LS time step t_1 to the subsequent LS time step t_2. Since the CRMs are laterally periodic, convective propagation can only occur as mediated by the LS model.

Neale (2011), who also demonstrate improvements on diurnal time scales.

d. Role of the dynamical core in the outer model

Pritchard and Somerville (2009a) showed no evidence of propagating systems in the central United States in their version of SP-CAM (SP-CAM3.0), which was run using a slightly different multiscale model configuration. At that time, we attributed this deficiency to the assumption of periodicity in the embedded cloud-system-resolving models. Revisiting our results (not shown), we found some evidence of propagating convective heating signatures, but nothing close to that reported herein for SP-CAM3.5. This is likely in part a resolution issue: in sensitivity tests with SP-CAM3.0 at higher spectral resolution (T85, or 175–350 km) we found evidence of propagating convective heating (latent heat release) in the lee of the Rockies, but no propagating rainfall signatures (not shown).

The further improvement reported here using SP-CAM3.5 in finite volume mode at comparable horizontal resolution (approximately 250 km) highlights the importance of the choice of dynamical core in the outer model. The grids on which large-scale and cloud-resolving model effects were computed in SP-CAM3.0 were inconsistent. Physics tendencies computed on the nonaliasing Gaussian grid in SP-CAM3.0 are not fully recognized by the spectral dynamics, which has fewer degrees of freedom. This may prevent latent heating that is barely resolved on the grid from realistically interacting with the spectral dynamics (D. Randall 2011, personal communication). Figure 17 illustrates this effect visually: A compact, localized 400-hPa diabatic heating anomaly induced by the embedded CRMs during event A in SP-CAM3.5 is horizontally interpolated using spectral routines to a 128×256 Gaussian grid, using triangular (T85) truncation. Although the Gaussian grid has higher ''resolution'' than the $1.9° \times 2.5°$ finite volume grid, the resulting heating anomaly is more diffuse, emphasizing that a spectral dynamical core cannot support the small-scale waves excited by localized heating anomalies in the finite volume model. While Fig. 15 depicts the cloud-resolving and large-scale models on an equivalent horizontal grid, this is only true for SP-CAM3.5 as a result of the finite volume dynamical core.

It is unknown to what extent the propagating signal in SP-CAM3.5 was enabled by increasing the horizontal resolution of the embedded CRM from 4 to 1 km. Existing documentation of the sensitivity of MMF simulations to varying the CRM grid spacing is insufficient to anticipate the effect of quadrupling CRM resolution on deep nocturnal U.S. convection. Marchand and Ackerman (2010) examine only low cloud mean

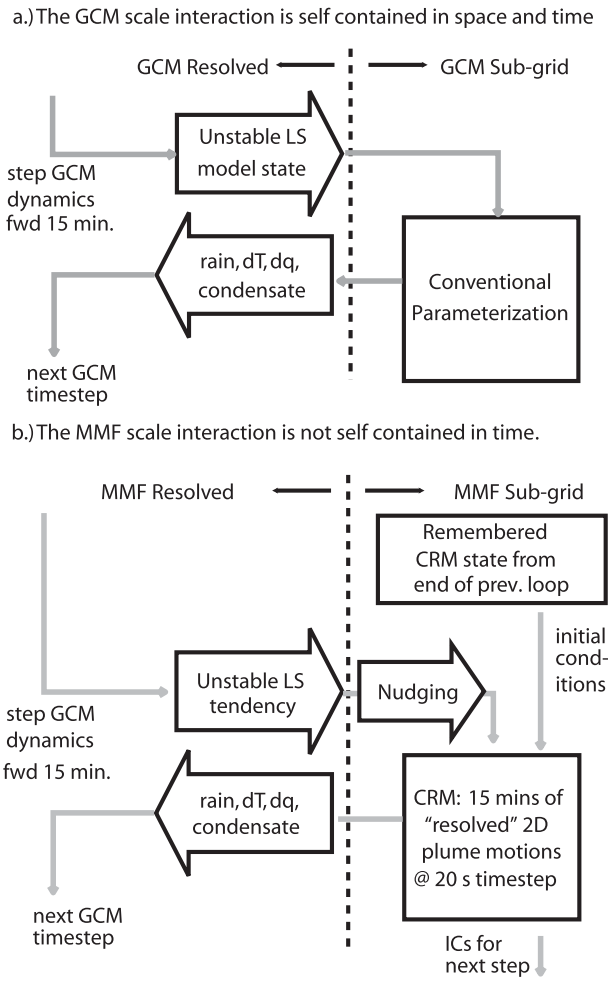

FIG. 16. Schematic illustrating how the scale interface in (a) GCMs is re-engineered in (b) the multiscale modeling framework (MMF) approach to global climate modeling. Light gray arrows define the code flow, and the vertical dashed line separates the resolved and subgrid scales. In the MMF approach, ''memory'' at the inner resolved scale plays a role in the subgrid response to large-scale forcing.

sensitivities to CRM resolution, and Khairoutdinov and Randall (2001) smooth their results with a 12-h filter. In the face of limited computing resources we chose the interior model resolution of 1 km to optimally admit key physics of 2D squall line organization based on the explicit CRM experience of Lafore and Moncrieff (1989) and Moncrieff and Liu (2006). The sensitivity of our result to this CRM resolution choice remains to be determined, and will be documented in future work.

7. Conclusions

Current generation global climate model projections of future hydrologic changes are especially uncertain in

the lee of mountain chains owing to deficiencies in conventional convective parameterization that were not designed to represent organized convective systems. This is strikingly apparent in the central United States where such systems account for much of the warm season climatological rainfall.

We have documented nocturnally persistent orogenic midlatitude warm season convection in the lee of the Rockies in a coarse-resolution global climate model that uses the embedded explicit convection approach to represent subgrid convection (i.e., a multiscale modeling framework). Analysis shows that the simulated propagating events in terms of propagation speed, synoptic forcing, and characteristic scale of the simulated events are within the observed range. Mean moisture content, stability of the Great Plains capping inversion, and mountain–plains solenoidal circulation are concurrently improved through the embedded cloud-resolving model approach. Storm-relative flow is realistically solenoidal at midtropospheric levels ahead of the simulated systems, but the simulated low-level penetrative easterly inflow is 2–4 times too deep.

In nature, propagating diurnal convective systems are also observed to occur over Africa, Indonesia, and South America, among other places. It is currently unknown if SPCAM3.5 can produce such tropical organized propagating diurnal convection—owing to the substantial data volume of the inner model, output for the simulation reported here was restricted to a North American subregion. Global output from the older spectral version of SP-CAM3.0 does not appear to contain propagating convection west of Colombia, or around the Indonesian islands, at either T42 or T85 horizontal resolution (not shown). But, since SP-CAM3.0 also did not admit significant central U.S. propagating convection, which has since turned out to exist in SP-CAM3.5, the question is still open for the time being: can the multiscale modeling approach admit propagating orogenic diurnal convection in the tropics where geostrophic dynamics have less control on scale interactions between the cloud-resolving model and large-scale grids?

Other issues associated with the organization of airflow in the evaporatively cooled (mesoscale) downdraft region remain to be understood. We encourage follow-on sensitivity studies of the nocturnal organized U.S. convection documented herein to clarify convective propagation mechanisms across the two resolved scales in the multiscale modeling approach. We have advocated that cloud-system-resolving simulations of organized convective heating project onto first-baroclinic gravity wave modes in the large-scale model, which in turn mediate dynamically consistent convective life cycle responses in nonlocal cloud-resolving models. However, other

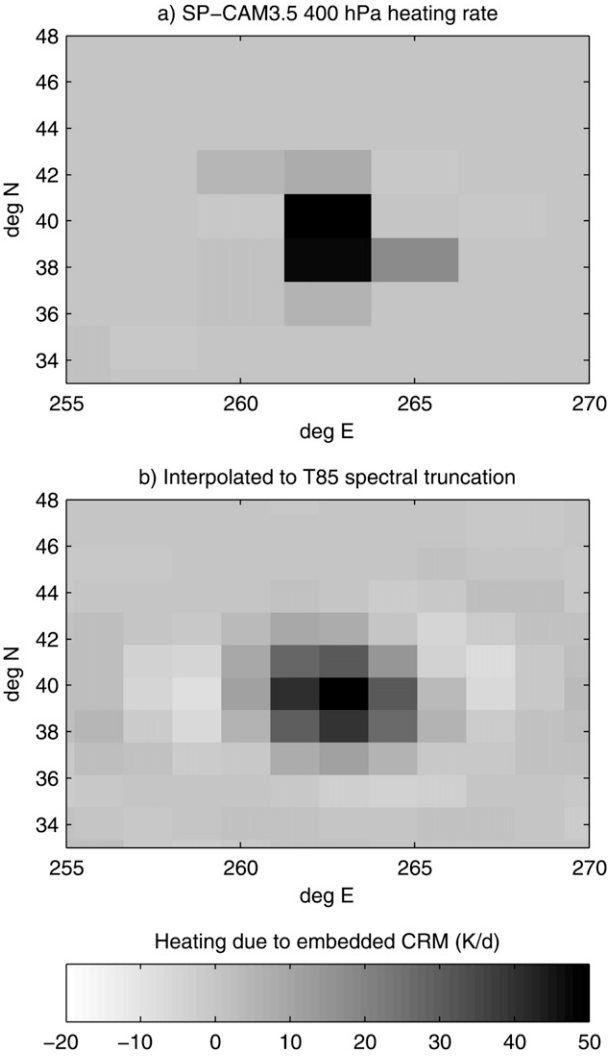

FIG. 17. (a) A snapshot showing the horizontal extent of the 400-hPa SP-CAM3.5 heating signature during a nocturnal propagating convective event on its $1.9° \times 2.5°$ finite volume horizontal grid. (b) Diffuse representation of the same field after spectral horizontal interpolation to triangular truncation at T85.

propagation mechanisms may exist within the possible multigrid degrees of freedom in multiscale modeling frameworks (e.g., large-scale advection of condensate or vapor anomalies impacting nonlocal cloud resolving model behavior via its total water equation). Further testing is needed that can discriminate between such mechanisms (e.g., with dual-grid water and energy budget calculations at the time resolution of scale coupling).

Limitations of the scope of this study open important new research questions in regard to the multiscale modeling approach, such as the following.

- Did the zonal orientation of the two-dimensional cloud-system-resolving models in our simulation optimize the

ability for SP-CAM3.5 to respond to the all-important effects of zonal shear in the lee of the Rockies on the propagating systems?
- To what extent would multigrid propagation have occurred if the 2D cloud-system-resolving models had been oriented meridionally?
- Should the fixed cloud-system-resolving model orientation be relaxed in MMFs—for example, through a random rotation of the 2D array to represent the 3D effects of large-scale wind shear on convective organization?
- Should the alignment be chosen in terms of dynamical criteria such as the mean vertical shear direction?
- To what extent was the propagating signal enabled by the increase in the horizontal resolution of the embedded explicit convection grid from 4 to 1 km?

A fundamental issue is the role of momentum transport by organized convection, which differs from the convective momentum transport parameterized in CAM3.5 as a mixing process that decreases shear. Organized convective momentum transport has the opposite effect—it can increase vertical shear in certain atmospheric layers (e.g., low-level shear, which is basic to mesoscale convective systems and their scale-interaction properties).

In the meantime, the broader implication of this paper is that multiscale modeling frameworks admit some of the missing diurnal physics of orogenic organized propagating convection over continents that are conspicuously absent from contemporary global climate models. With additional understanding and refinement the multiscale approach to climate modeling may one day help improve longer-term hydrologic climate forecasts in heavily populated parts of the world where diurnal physics project onto climate time scales and conventional climate model projections disagree.

Acknowledgments. This research was supported by the Center for Multiscale Modeling of Atmospheric Processes (CMMAP), a National Science Foundation (NSF) Science and Technology Center managed by Colorado State University under Cooperative Agreement ATM-0425247 with computing support from NSF TeraGrid (TG-ATM090002). NSF sponsors the National Center for Atmospheric Research. This research was also supported in part by the U.S. Department of Energy (DOE)'s Atmospheric Science Program Atmospheric System Research, an Office of Science, Office of Biological and Environmental Research program, under Grant DE-FG02-09ER64764 and DOE Grant DE-SC0002003. SP-CAM3.5 was generously developed by Marat Khairoutdinov. We are grateful to John Helly, Guang Zhang, David Randall, Chris Bretherton, Eric Maloney, Roger Marchand, Gabe Kooperman, Greg Elsaesser, Steve Ghan, Kate Thayer-Calder, Jim Benedict, Peter Blossey, and two anonymous reviewers for insightful feedback during this work.

REFERENCES

Benedict, J. J., and D. A. Randall, 2009: Structure of the Madden–Julian oscillation in the superparameterized CAM. *J. Atmos. Sci.,* **66,** 3277–3296.

Carbone, R. E., and J. D. Tuttle, 2008: Rainfall occurrence in the U.S. warm season: The diurnal cycle. *J. Climate,* **21,** 4132–4146.

——, ——, D. Ahijevych, and S. B. Trier, 2002: Inferences of predictability associated with warm season precipitation episodes. *J. Atmos. Sci.,* **59,** 2033–2056.

Collins, W., and Coauthors, 2004: Description of the NCAR community atmosphere model (CAM 3.0). NCAR Tech. Note NCAR/TN-464+ STR, 210 pp.

Correia, J., R. W. Arritt, and C. J. Anderson, 2008: Idealized mesoscale convective system structure and propagation using convective parameterization. *Mon. Wea. Rev.,* **136,** 2422–2442.

DeMott, C. A., D. A. Randall, and M. Khairoutdinov, 2007: Convective precipitation variability as a tool for general circulation model analysis. *J. Climate,* **20,** 91–112.

Dirks, R. A., 1969: A theoretical investigation of convective patterns in the lee of the Rockies. Ph.D. thesis, Colorado State University, 134 pp.

Ghan, S., X. Bian, and L. Corsetti, 1996: Simulation of the Great Plains low-level jet and associated clouds by general circulation models. *Mon. Wea. Rev.,* **124,** 1388–1408.

Grabowski, W. W., and P. K. Smolarkiewicz, 1999: CRCP: A cloud resolving convection parameterization for modeling the tropical convecting atmosphere. *Physica D,* **133,** 171–178.

——, and M. W. Moncrieff, 2001: Large-scale organization of tropical convection in two-dimensional explicit numerical simulations. *Quart. J. Roy. Meteor. Soc.,* **127,** 445–468.

Houze, R., 2004: Mesoscale convective systems. *Rev. Geophys.,* **42,** RG4003, doi:10.1029/2004RG000150.

Jiang, X., N.-C. Lau, and S. A. Klein, 2006: Role of eastward propagating convection systems in the diurnal cycle and seasonal mean of summertime rainfall over the U.S. Great Plains. *Geophys. Res. Lett.,* **33,** L19809, doi:10.1029/2006GL027022.

Jirak, I. L., and W. R. Cotton, 2007: Observational analysis of the predictability of mesoscale convective systems. *Wea. Forecasting,* **22,** 813–838.

Khairoutdinov, M. F., and D. A. Randall, 2001: A cloud resolving model as a cloud parameterization in the NCAR Community Climate System Model: Preliminary results. *Geophys. Res. Lett.,* **28,** 3617–3620.

——, and ——, 2003: Cloud resolving modeling of the ARM summer 1997 IOP: Model formulation, results, uncertainties, and sensitivities. *J. Atmos. Sci.,* **60,** 607–625.

——, D. Randall, and C. DeMott, 2005: Simulations of the atmospheric general circulation using a cloud-resolving model as a superparameterization of physical processes. *J. Atmos. Sci.,* **62,** 2136–2154.

——, C. DeMott, and D. Randall, 2008: Evaluation of the simulated interannual and subseasonal variability in an AMIP-style

simulation using the CSU multiscale modeling framework. *J. Climate,* **21,** 413–431.

Kingsmill, D. E., and R. A. Houze, 1999: Kinematic characteristics of air flowing into and out of precipitating convection over the west Pacific warm pool: An airborne Doppler radar survey. *Quart. J. Roy. Meteor. Soc.,* **125,** 1165–1207.

Lafore, J., and M. Moncrieff, 1989: A numerical investigation of the organization and interaction of the convective and stratiform regions of tropical squall lines. *J. Atmos. Sci.,* **46,** 521–544.

Laing, A. G., and J. M. Fritsch, 1997: The global population of mesoscale convective complexes. *Quart. J. Roy. Meteor. Soc.,* **123,** 389–405.

——, and ——, 2000: The large-scale environments of the global populations of mesoscale convective complexes. *Mon. Wea. Rev.,* **128,** 2756–2776.

Lee, M.-I., S. D. Schubert, M. J. Suarez, J.-K. E. Schemm, H.-L. Pan, J. Han, and S.-Y. Yoo, 2008: Role of convection triggers in the simulation of the diurnal cycle of precipitation over the United States Great Plains in a general circulation model. *J. Geophys. Res.,* **113,** D02111, doi:10.1029/2007JD008984.

Li, Y., and R. B. Smith, 2010: The detection and significance of diurnal pressure and potential vorticity anomalies east of the Rockies. *J. Atmos. Sci.,* **67,** 2734–2751.

Maddox, R. A., 1983: Large-scale meteorological conditions associated with midlatitude, mesoscale convective complexes. *Mon. Wea. Rev.,* **111,** 1475–1493.

Mapes, B. E., and R. B. Neale, 2011: Parameterizing convective organization to escape the entrainment dilemma. *J. Adv. Model. Earth Syst.,* **3,** M06004, doi:10.1029/2011MS000042.

Marchand, R., and T. Ackerman, 2010: An analysis of cloud cover in multiscale modeling framework global climate model simulations using 4 and 1 km horizontal grids. *J. Geophys. Res.,* **115,** D16207, doi:10.1029/2009JD013423.

——, J. Haynes, G. G. Mace, T. Ackerman, and S. G. Graeme, 2009: A comparison of simulated cloud radar output from the multiscale modeling framework global climate model with CloudSat cloud radar observations. *J. Geophys. Res.,* **114,** D00A20, doi:10.1029/2008JD009790.

Matsui, T., D. Mocko, M.-I. Lee, W.-K. Tao, M. J. Suarez, and R. A. Pielke Sr., 2010: Ten-year climatology of summertime diurnal rainfall rate over the conterminous U.S. *Geophys. Res. Lett.,* **37,** L13807, doi:10.1029/2010GL044139.

Moncrieff, M. W., 1981: A theory of organized steady convection and its transport properties. *Quart. J. Roy. Meteor. Soc.,* **107,** 29–50.

——, 1992: Organized convective systems: Archetypal dynamical models, mass and momentum flux theory, and parametrization. *Quart. J. Roy. Meteor. Soc.,* **118,** 819–850.

——, 2010: The multiscale organization of moist convection at the intersection of weather and climate. *Why Does Climate Vary? Geophys. Monogr.,* Vol. 189, Amer. Geophys. Union, 3–26.

——, and C. H. Liu, 2006: Representing convective organization in prediction models by a hybrid strategy. *J. Atmos. Sci.,* **63,** 3404–3420.

Pandya, R. E., and D. R. Durran, 1996: The influence of convectively generated thermal forcing on the mesoscale circulation around squall lines. *J. Atmos. Sci.,* **53,** 2924–2951.

Pritchard, M. S., and R. C. J. Somerville, 2009a: Assessing the diurnal cycle of precipitation in a multi-scale climate model. *J. Adv. Model. Earth Syst.,* **1,** 12, doi:10.1029/JAMES.2009.1.12.

——, and ——, 2009b: Empirical orthogonal function analysis of the diurnal cycle of precipitation in a multi-scale climate model. *Geophys. Res. Lett.,* **36,** L05812, doi:10.1029/2008GL036964.

Randall, D., M. Khairoutdinov, A. Arakawa, and W. Grabowski, 2003: Breaking the cloud parameterization deadlock. *Bull. Amer. Meteor. Soc.,* **84,** 1547–1564.

Raymond, D., and H. Jiang, 1990: A theory for long-lived mesoscale convective systems. *J. Atmos. Sci.,* **47,** 3067–3077.

Rotunno, R., J. Klemp, and M. Weisman, 1988: A theory for strong, long-lived squall lines. *J. Atmos. Sci.,* **45,** 463–485.

Stan, C., M. Khairoutdinov, C. A. DeMott, V. Krishnamurthy, D. M. Straus, D. A. Randall, J. L. Kinter, and J. Shukla, 2010: An ocean–atmosphere climate simulation with an embedded cloud-resolving model. *Geophys. Res. Lett.,* **37,** L01702, doi:10.1029/2009GL040822.

Tao, W., and M. Moncrieff, 2009: Multiscale cloud system modeling. *Rev. Geophys.,* **47,** RG4002, doi:10.1029/2008RG000276.

Thorpe, A., M. Miller, and M. Moncrieff, 1980: Dynamical models of two-dimensional downdraughts. *Quart. J. Roy. Meteor. Soc.,* **106,** 463–484.

Trier, S. B., C. A. Davis, D. A. Ahijevych, M. L. Weisman, and G. H. Bryan, 2006: Mechanisms supporting long-lived episodes of propagating nocturnal convection within a 7-day WRF model simulation. *J. Atmos. Sci.,* **63,** 2437–2461.

——,——, and ——, 2010: Environmental controls on the simulated diurnal cycle of warm-season precipitation in the central United States. *J. Atmos. Sci.,* **67,** 1066–1090.

Tripoli, G. J., and W. R. Cotton, 1989: Numerical study of an observed orogenic mesoscale convective system. Part 1: Simulated genesis and comparison with observations. *Mon. Wea. Rev.,* **117,** 273–304.

Tuttle, J. D., and C. A. Davis, 2006: Corridors of warm season precipitation in the central United States. *Mon. Wea. Rev.,* **134,** 2297–2317.

Zhang, G. J., and N. A. McFarlane, 1995: Sensitivity of climate simulations to the parameterization of cumulus convection in the Canadian Climate Centre general circulation model. *Atmos.–Ocean,* **33,** 407–446.

Zhang, Y., and Coauthors, 2008: On the diurnal cycle of deep convection, high-level cloud, upper troposphere water vapor in the multiscale modeling framework. *J. Geophys. Res.,* **113,** D16105, doi:10.1029/2008JD009905.